

Errors of New Transformer Converters Measuring Angular Displacement Difference

Sultan Amirov¹ and Nurulla Yuldashev²

¹Tashkent State Transport University, Temiryulchilar Str. 1, 100167 Tashkent, Uzbekistan

²University of Tashkent for Applied Sciences, Gavhar Str. 1, 100149 Tashkent, Uzbekistan

Iscmmstiai2022@gmail.com, yuldashevn@gmail.com

Keywords: Angular Displacement, Angular Displacement Difference, Transformer Converter, Error Sources, Main Error, Additional Error, Magnetic Circuit, Drive Coil, Measuring Coil, Load Resistance, Regular Error, Random Error.

Abstract: The article identifies and evaluates the error sources of transformer converters designed to measure the angular displacements of two objects in the newly developed and automatic control and management systems and their difference. Analysis of error sources showed that their theoretical, technological, and operational sources are the main error sources, while internal, external, and mode sources are additional error sources. Theoretical sources of error usually arise from the fact that the measuring device being studied is not taken into account in full all the laws in its work activities, and technological sources are from the fact that the technology for making a measuring device has not been improved. Errors that arise in the process of assembling and configuring the structure are also included in the sources of technological error. The error due to the nonlinearity of the static characteristics of the new transformers is greater than other main error sources, the errors due to changes in the amplitude, frequency and load resistance of the excitation current are greater than other additional error sources, and the calculated errors of the two new transformers 5% and 1.0%, respectively.

1 INTRODUCTION

It is known that, depending on the value of the error of a measuring transducer (MT), its metrological capabilities and accuracy class are determined, as well as its areas of application [1], [2].

Therefore, in this article, we study the error characteristics of two new MT transformers (TOO), developed at Tashkent State University of Transport and intended for use in technological processes and production control and management systems, measuring the angular displacements of two objects and their difference. We do not dwell in detail on the design schemes, operating principles, and specific features of the new transformer devices, as these are described in sources [3], [4].

It is known [5] that the main sources of error of the TOO under normal operating conditions (when the current or voltage supplied to the excitation coil is nominal, the waveform is sinusoidal, the frequency is moderate, the ambient temperature is normal, external electric and magnetic fields as well as ferromagnetic masses are absent, all derivatives

of the order are equal to zero, and the output load is constant) constitute the intrinsic error sources. Additional sources of error include those that arise when the MT deviates from normal operating conditions.

2 METHODS

The new transformer MTs, which measure the difference in angular displacements, are the main sources of error.

2.1 Sources of Theoretical Errors

2.1.1 Error Caused by Nonlinearity of MT Static Characteristic

It is known that [6] when using OOs with nonlinear static characteristics in automatic control systems, due to the nonlinearity of the static characteristics,

the amount of error equal to the degree of nonlinearity of the static characteristics.

The error due to the nonlinearity of the static characteristic of MT is calculated using the following [7]:

$$\gamma_\varepsilon = \frac{U_{e.out.(\Delta Q_M = \Delta Q_{M.*})} - \Delta Q_{M.*} \frac{U_{e.out.(\Delta Q_M = \Delta Q_{M.max})}}{\Delta Q_{M.max}}}{2U_{e.out.(\Delta Q_M = \Delta Q_{M.max})}} \cdot 50 \%, \quad (1)$$

Where is $\Delta Q_{M.*}$ - the static characteristic of the difference in the angles of rotation of the moving parts is the relative value of the coordinate when the degree of nonlinearity is greatest.

We calculate the value of this error in the example of TOO, which is determined by the function given in the analytical expression of the static characteristic [4] and whose construction is given in [3]. To do this, the static characteristic function $\Delta Q_M = \Delta Q_{M.*}$ ва $\Delta Q_M = \Delta Q_{M.max}$ Substituting the values in (1) into the (2), we obtain the following:

$$\gamma_\varepsilon = \frac{3K_1^2(\Delta Q_{M.max})^2}{4K_1^2(\Delta Q_{M.max})^2 - 16W_{\mu\delta_{w0}}^2} \cdot 50 \%, \quad (2)$$

Where is K_1 – a coefficient depending on the magnetic properties and geometric dimensions of the working air gap, $[1/(H \cdot \text{degri})]$; $W_{\mu\delta_{w0}}$ – the value of the magnetic resistance of the working air gap when the TOO moving parts are in the neutral position. $[1/H]$.

Equation (2) analysis shows that the magnetic stiffness of the working air gap under study (mainly working air space $\delta_{w.0}$) The value of γ_ε decreases with increasing value. For example, if $\delta_{w.0} = 1,0 \text{ mm}$ $\gamma_\varepsilon = 2,67 \%$, $\delta_{w.0} = 2,0 \text{ mm}$ in this case will be $\gamma_\varepsilon = 1,09 \%$. It should be noted that the degree of nonlinearity of the static characteristic is zero when the input size of the new TOO operates in the $0 \div 0.4$ part of the entire working range.

2.1.2 Error Due to Reactive Component of Magnetic Resistance

An error caused by the reactive component of the magnetic resistance of an MD magnetic conductor. The complex magnetic resistance of the steel core causes the TOO to change the phase of the output signal depending on the difference in angular displacements at its input. We create a new static characteristic complex expression of the complex expression in the following form, divided into real and abstract parts:

$$U_{e.out.}^* = \frac{K_{12}}{K_1} * \frac{(W_{\mu\delta_{w0}}^2 - K_{12}^2(\Delta Q_M)^2)(W_{\mu1}^2 - K_{12}^2(\Delta Q_M)^2)}{(W_{\mu1}^2 - K_{12}^2(\Delta Q_M)^2)^2 + W_{\mu2}^4} + +j \frac{K_{12}}{K_1} * \frac{(W_{\mu\delta_{w0}}^2 - K_{12}^2(\Delta Q_M)^2)W_{\mu2}^2}{(W_{\mu1}^2 - K_{12}^2(\Delta Q_M)^2)^2 + W_{\mu2}^4} \quad (3)$$

Where $W_{\mu1}^2 = W_{\mu\delta_{w0}}^2 + 3W_{\mu\pi a}^2 + W_{\mu\pi p}^2 + 4W_{\mu\delta_{w0}}W_{\mu\pi a}$; $W_{\mu2}^2 = 4W_{\mu\pi a}W_{\mu\delta_{w0}} + 6W_{\mu\pi p}W_{\mu\pi a}$; $W_{\mu\pi a}$, $W_{\mu\pi p}$ – active and reactive resistances of the magnetic resistance ($W_{\mu\pi}$) of magnetic conductors made of electrotechnical steel, respectively, $[1/H]$; $K_{12} = K_1 + K_2$; K_2 – coefficient depending on the magnetic properties and geometric dimensions of magnetic conductors made of electrical steel, $[1/(H \cdot \text{degri})]$.

The change in the phase of the output signal depending on the coordinates of the moving parts of the TOO is determined by the following:

$$\arctg \frac{\varphi_{e.out.}}{W_{\mu\delta_{w0}}^2 + 3W_{\mu\pi a}^2 + W_{\mu\pi p}^2 + 4W_{\mu\delta_{w0}}W_{\mu\pi a} - K_{12}^2(\Delta Q_M)^2} = \frac{4W_{\mu\pi p}W_{\mu\delta_{w0}} + 6W_{\mu\pi p}W_{\mu\pi a}}{\varphi_{e.out.}} \quad (4)$$

The phase error is calculated using the following (5) based on the methodology presented in [8]:

$$\gamma_{\varphi_{e.out.}} = \frac{[tg\varphi_{e.out.}(\Delta Q_M = \Delta Q_{M.max}) - tg\varphi_{e.out.}(\Delta Q_M = 0)]}{-tg\varphi_{e.out.}(\Delta Q_M = 0)} \cdot 100 \%. \quad (5)$$

In a magnetic conductor (at $f=50 \text{ Hz}$) collected from thin steel cans, typically, will be $(W_{\mu\pi p}/W_{\mu\pi a}) = 0,3 \div 1,0$ [9]. The value calculated by (5) for the dimensions and design parameters of the new TOO made when this ratio is equal to 0.6 $\gamma_{\varphi_{e.out.}} = 0,063 \%$ is formed.

2.1.3 Effect of High Harmonics in TOO Output Voltage

The proportion of high harmonics in the output voltage of the TOO. The high harmonic constituents in the TOO output signal occur due to the nonlinearity of the magnetic characteristics of the steel core in the magnetic chain [10]. Analysis of theoretical and experimental studies in this area shows that only the third harmonic has a significant effect from the high harmonic constituents in the signal composition [11]. Therefore, we are also limited to determining the effect of this third harmonic on the magnitude of the TOO output signal. For this, Professor Zaripov M.F. We use the method of harmonic analysis, proposed by and effective for transformer OOs with a moving part [7]. This method is based on the approximation

of the magnetic characteristics of any nonlinear section of a magnetic chain using two functions simultaneously.

Given that there are working air gaps in the path of the working magnetic fluxes in the magnetic chains of the studied arrows, we use the following pair of proposed functions to approximate the magnetic characteristics for the regime in which the saturation level of the steel core is not strong [7]:

$$H = aB - bB^3 = 1,5 \frac{H_M}{B_M} B - 0,5 \frac{H_M}{B_M^3} B^3, \quad (6)$$

$$B = cH + dH^3 = 0,5 \frac{B_M}{H_M} H + 0,5 \frac{B_M}{H_M^3} H^3, \quad (7)$$

Where is a , b , c and d – approximation coefficients; B_M , H_M – are the maximum values of induction and voltage, which are usually calculated without taking into account the resistance of the magnetic conductor (steel core) part of the magnetic circuit [12].

The simplified exchange scheme of the TOO magnetic chain is based on its steel core part and working air gaps, respectively $W_{\mu n}$ and $W_{\mu \delta} = \frac{2\delta}{\mu_0 S_{\mu n}}$ consists of a series connection of resistors (Fig. 1).

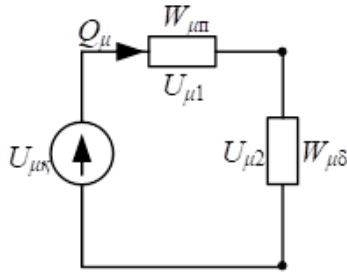


Figure 1: Simplified exchange scheme of the new TOO magnetic circuit.

The magnetic characteristics of the steel core (nonlinear) part of the magnetic chain are its cross-sectional surface $S_{\mu n}$ and length equals to $l_{\mu n}$ and $H_1 = \frac{U_{\mu 1}}{l_{\mu n}}$ and $B_1 = \frac{Q_{\mu}}{S_{\mu n}}$ on the basis of (6) and (7), taking into account the relationship is written as follows:

$$U_{\mu 1} = 1,5 \frac{l_{\mu n}}{S_{\mu n}} \cdot \frac{H_M}{B_M} Q_{\mu} - 0,5 \frac{l_{\mu n}}{S_{\mu n}^3} \cdot \frac{H_M}{B_M^3} Q_{\mu}^3, \quad (8)$$

$$Q_{\mu} = 0,5 \frac{S_{\mu n}}{l_{\mu n}} \cdot \frac{B_M}{H_M} U_{\mu 1} + 0,5 \frac{S_{\mu n}}{l_{\mu n}^3} \cdot \frac{B_M}{H_M^3} U_{\mu 1}^3. \quad (9)$$

Ere is Q_{μ} – magnet current, [Wb].

The magnetic characteristics of the air gaps (linear) part of the magnetic chain are written as follows:

$$U_{\mu 2} = Q_{\mu} W_{\mu \delta}. \quad (10)$$

The first equation of the magnetic characteristic of the whole magnetic chain is written as follows on the basis of Kirchhoff's 2nd law:

$$U_{\mu \kappa} = U_{\mu 12} = U_{\mu 1} + U_{\mu 2} = \left(1,5 \frac{l_{\mu n}}{S_{\mu n}} \cdot \frac{H_M}{B_M} + W_{\mu \delta} \right) Q_{\mu} - 0,5 \frac{l_{\mu n}}{S_{\mu n}^3} \cdot \frac{H_M}{B_M^3} Q_{\mu}^3 = a_{12} Q_{\mu} - b_{12} Q_{\mu}^3, \quad (11)$$

$$\text{Where is } a_{12} = \left(1,5 \frac{l_{\mu n}}{S_{\mu n}} \cdot \frac{H_M}{B_M} + W_{\mu \delta} \right), [A/Wb];$$

$$b_{12} = 0,5 \frac{l_{\mu n}}{S_{\mu n}^3} \cdot \frac{H_M}{B_M^3}, [A/(Wb)^3].$$

The coefficients c_{12} and d_{12} , found on the basis of the method given in the second magnetic characteristic of the magnetic chain [7], are equal to:

$$c_{12} = \frac{2Q_{\mu M} U_{\mu M} - \left(1,5 \frac{l_{\mu n}}{S_{\mu n}} \cdot \frac{H_M}{B_M} + W_{\mu \delta} \right) Q_{\mu M}^2}{U_{\mu M}^2}, \quad (12)$$

$$d_{12} = \frac{\left(1,5 \frac{l_{\mu n}}{S_{\mu n}} \cdot \frac{H_M}{B_M} + W_{\mu \delta} \right) Q_{\mu M}^2 - Q_{\mu M} U_{\mu M}}{U_{\mu M}^4}. \quad (13)$$

The second magnetic characteristic of the magnetic chain, taking into account (12) and (13), is written in the following form:

$$Q_{\mu} = c_{12} U_{\mu 12} + d_{12} U_{\mu 12}^3. \quad (14)$$

When the MD excitation coil under study is supplied from a sinusoidal current source, the MMP in the magnetic circuit is recorded as follows:

$$U_{\mu \kappa} = U_{\mu 12} = i_{\kappa} w_{\kappa n} \Delta Q_M = I_{\kappa M} w_{\kappa n} \Delta Q_M \sin \omega_e t. \quad (15)$$

Equation (15) substituting (14) and using the appropriate trigonometric accuracy, we obtain the following expression for the working magnetic flux crossing the measuring coil:

$$Q_{\mu w.} = \left\{ c_{12} I_{\kappa M} w_{\kappa n} \Delta Q_M + \frac{3}{4} d_{12} (I_{\kappa M} w_{\kappa n} \Delta Q_M)^3 \right\} \sin \omega_e t - \frac{d_{12}}{4} (I_{\kappa M} w_{\kappa n} \Delta Q_M)^3 \sin 3\omega_e t. \quad (16)$$

The EMF that induces the working magnetic flux in the measuring coil is as follows:

$$e_{out.} = -w_{meas.} \frac{dQ_{\mu w.}}{dt} = -w_{meas.} \omega_e \left[c_{12} I_{\kappa M} w_{\kappa n} \Delta Q_M + \frac{3}{4} d_{12} (I_{\kappa M} w_{\kappa n} \Delta Q_M)^3 \right] \cos \omega_e t + \frac{3}{4} w_{meas.} \omega_e d_{12} (I_{\kappa M} w_{\kappa n} \Delta Q_M)^3 \cos 3\omega_e t = -E_{out.1m} \cos \omega_e t + E_{out.3m} \cos 3\omega_e t. \quad (17)$$

The ratio of the 3- and 1-harmonics of the output EMF is as follows:

$$\frac{E_{out.3m}}{E_{out.1m}} = \frac{3[a_{12}Q_{\mu m} - U_{\mu m}](I_{km}w_{k\alpha}\Delta Q_M)^2}{4[2Q_{\mu m}U_{\mu m} - a_{12}]Q_{\mu m}U_{\mu m}^2 + 3[a_{12}Q_{\mu m} - U_{\mu m}](I_{km}w_{k\alpha}\Delta Q_M)^2}, \quad (18)$$

The proportion of 3-harmonics relative to 1-harmonics did not exceed 4.8% for the mode in which the saturation level of the steel core was not strong in the parameters of the electric and magnetic chains of the constructed TOO under study. The most convenient way to reduce this proportion is to ensure that the steel core part of the magnetic chain operates in a straight line section of the magnetization characteristic.

2.2 Sources of Technological Errors

2.2.1 Non-Constant Magnetic Resistance Error

The error caused by the magnetic resistance of the magnetic conductor is not constant. The error due to the fact that the magnetic resistance of the magnetic conductor is not constant along the magnetic chain due to technological reasons as noted [7], [8], [11], the negligibility is very small. We therefore assume that there is no need to derive the analytical equation of this error.

2.2.2 Non-Uniform Winding Distribution Error

The slope distribution is not a constant pogan value. In the TOOs under study, the excitation coils are required to be wrapped in a uniformly distributed form in the appropriate parts of the magnetic chain. However, there is an error in step (α) of winding the twisted wires when carrying out this technological process ($\Delta\alpha$) ka can be allowed. This error is determined using the following (19) [13]:

$$\Delta\alpha = k_\alpha\alpha. \quad (19)$$

Where is k_α – a coefficient that depends on the accuracy class of the wire wrapping equipment.

Length $\Delta\alpha = \alpha_0$ The number of windings of the excitation coil located in the magnetic conductor, which is:

$$w_{k,\alpha} \approx w_{k,\alpha_0} + \Delta w_{k,\alpha}. \quad (20)$$

The magnetic flux associated with a coil with a uniform distribution of windings and a length l can be found using the following:

$$\Psi = \sum_0^{\alpha} w_{k,\alpha} Q_\mu. \quad (21)$$

Taking into account the EMF (21) at the output of the TOO under study, it is determined as follows:

$$\dot{E}_{out.} = - \frac{j\omega I_{ek}w_k w_{meas.}}{(\frac{1}{4}Z_{\mu r} + Z_{\mu d})\Delta Q_{Mmax}} \left(w_{k,\alpha}\Delta Q_M \pm \sum_0^{\alpha} \Delta w_{k,\alpha} \right). \quad (22)$$

If we take into account that each value of $\Delta w_{k,\alpha}$ occurs under the influence of random causes, then the sum value of $\Delta w_{k,\alpha}$ can be determined in the form of the following quadratic error:

$$\sum_0^{\alpha} \Delta w_{k,\alpha} = \frac{\sigma}{\sqrt{\alpha_0}}. \quad (23)$$

Here is σ – is the variance, and for the case we are studying it is equal to k_α

The root expression of (23) when the number of layers of windings in the winding is $\frac{n\alpha}{\alpha_0}$ is written in appearance. Thus, (22) is written as follows:

$$\dot{E}_{out.} = - \frac{j\omega I_{ek}w_k w_{meas.}\Delta Q_M}{(\frac{1}{4}Z_{\mu r} + Z_{\mu d})\Delta Q_{Mmax}} \left(1 \pm \frac{k_\alpha}{w_{k,\alpha}\Delta Q_M} \sqrt{\frac{\alpha_0}{n\alpha}} \right) = \dot{E}_{out.0} + \Delta \dot{E}_{out.}. \quad (24)$$

The error due to the instability of the pogan value of the excitation ring distribution is found as follows:

$$\gamma_{w_{k,\alpha}} = \frac{\Delta E_{out.}}{E_{out.max}} = \frac{k_\alpha}{w_{k,\alpha}\Delta Q_{Mmax}} \sqrt{\frac{\alpha_0}{n\alpha}}. \quad (25)$$

If we consider that the maximum value of the error occurs at $\alpha = \alpha_0$, then (25) is in the following form:

$$\gamma_{w_{k,\alpha}} = \frac{\Delta E_{out.}}{E_{out.max}} = \frac{k_\alpha}{w_{k,\alpha}\Delta Q_{Mmax}\sqrt{n}}. \quad (26)$$

Thus, the error due to the non-constant pogan value of the drive winding distribution is n, the number of layers of windings in it, the angle of rotation of the moving part and the pogan values n of the windings of scattered windings are small.

2.2.3 Assembly and Adjustment Errors

Errors due to inaccuracies in the assembly and adjustment of the structure. For example, when installing magnetic conductors in the form of a spiral, which is one of the moving parts of the new TOO, the initial values of the working air gaps are correspondingly $(\delta_{w,0} + \Delta)$ and equas to $(\delta_{w,0} - \Delta)$. In this case TOO working air gaps for magnetic stiffness $W_{\mu\delta'w\Sigma} = W_{\mu\delta_{w,0}} + \Delta W_{\mu\delta_{w,0}}$ and we will have $W_{\mu\delta''w\Sigma} = W_{\mu\delta_{w,0}} - \Delta W_{\mu\delta_{w,0}}$. For this

case, the output EMF in the measuring tube is equal to:

$$U_{e.out.} = \frac{2\omega j_{ek} W_k W_{meas.} (\Delta W_{\mu\delta_{w0}} + K_1 \Delta Q_M)}{W_{\mu\delta_{w0}}^2 - (\Delta W_{\mu\delta_{w0}})^2 - \Delta W_{\mu\delta_{w0}} K_1 \Delta Q_M - K_1^2 (\Delta Q_M)^2}. \quad (27)$$

The resulting error due to inaccuracies in the assembly and adjustment of the TOO design is calculated as follows:

$$\gamma_{amoun} = \frac{U_{e.out.} - U_{e.out.0}}{U_{e.out.0} (\Delta Q_{Mmax})} \cdot 100 \% = \frac{W_{\mu\delta_{w0}}^2 \Delta W_{\mu\delta_{w0}} + K_1 \Delta Q_M (\Delta W_{\mu\delta_{w0}})^2}{(W_{\mu\delta_{w0}}^2 - (\Delta W_{\mu\delta_{w0}})^2 - \Delta W_{\mu\delta_{w0}} K_1 \Delta Q_M - K_1^2 (\Delta Q_M)^2) (W_{\mu\delta_{w0}}^2 - K_1^2 (\Delta Q_M)^2)} \cdot \frac{(W_{\mu\delta_{w0}}^2 - (\Delta W_{\mu\delta_{w0}})^2 - \Delta W_{\mu\delta_{w0}} K_1 \Delta Q_{Mmax} - K_1^2 (\Delta Q_{Mmax})^2)}{(\Delta W_{\mu\delta_{w0}} + K_1 \Delta Q_{Mmax})} \cdot 100 \%. \quad (28)$$

Where is $U_{e.out.0}$ – the value of the output voltage in the absence of uncertainties in the assembly and adjustment; $U_{e.out.0} (\Delta Q_{Mmax})$ – (27) value in $\Delta Q_M = \Delta Q_{Mmax}$.

For the construction parameters of the new TOO $\Delta W_{\mu\delta_{w0}} = 0,05 W_{\mu\delta_{w0}}$ when $\gamma_{amoun} = 0,033 \%$.

2.3 Operational Error Sources

Sources of this type of error are subject to the axioms of randomness, and the laws of their occurrence depend only on the operational characteristics [14].

2.3.1 Working Air Gap Backlash Error

Luft of working air gap. According to the (29) formed in the working air gap luft [7] for the newly developed TOO is determined as follows:

$$\gamma_l = \frac{x}{x_M} \cdot \frac{(\Delta l)^2}{(\delta_{w.0})^2}. \quad (29)$$

Where is x , x_M Linear displacement of the moving part of the bullet and its maximum value; Δl is the backlash measurement.

2.3.2 Mechanical Hysteresis Error

Mechanical hysteresis is caused by the formation of a bend (perekos) due to the fact that the moving part of the TOO is not firmly connected with the controlled object [13]. The error due to mechanical hysteresis in the TOO, which measures the difference in angular displacements, is generally found using the following (30):

$$\gamma_{mech.hys} = \pm \frac{\delta Q_M}{\Delta Q_{Mmax}} \%. \quad (30)$$

Where is δQ_M – the angle of lag in the direction of rotation of the moving part due to mechanical hysteresis.

For the new TOO under study, when $\delta Q_M = \pm 0,4 \text{ degri}$ and $\Delta Q_{Mmax} = 85 \text{ degri}$ when forms $\gamma_{mech.hys} = \pm 0,005 \%$.

2.3.3 Magnetic Hysteresis Error

Magnetic hysteresis- is a function of the dependence of the working magnetic flux on the difference in the coordinates of the moving parts, since the magnetic characteristic of the steel core in the magnetic chain under study is in the form of a hysteresis surface. [14]. The maximum value of the error due to magnetic hysteresis is determined by the maximum width of the magnetic field along the axis of tension of the hysteresis rod, and it is calculated using the following (31) [15]:

$$\gamma_{mag.hys.(max)} = \pm \frac{H_{res.} W_{\mu n} C_{\mu\delta_w}}{H_{max}} \%. \quad (31)$$

Where is H_{max} , $H_{res.}$ – maximum and residual values of stresses in the steel core; $W_{\mu n}$, $C_{\mu\delta_w}$ – the magnetic resistance (magnetic hardness) of the steel core in the working magnetic flux path and the conductivity of the working air gap (magnetic capacity). $\frac{H_{res.}}{H_{max}} = 0,1$ The value of $\gamma_{mag.hys.(max)}$ for the TOO under study does not exceed 0.0015%.

2.3.4 Component Wear Error

Obsolescence of TOO details. As a result of the wear of the parts, the wear of the friction surfaces of the moving and non-moving parts of the TOO during operation causes additional backlash. In addition, the wear of the magnetic material also leads to a change in its magnetic characteristics. In this case (31) $W_{\mu n} C_{\mu\delta_w}$, the larger the multiplication, the greater the error caused by the change in the magnetic characteristic.

New transformer converters that measure angular displacement difference are additional error sources.

2.4 Internal Additional Error Sources

2.4.1 Excitation Coil Voltage/Current Amplitude Error

An error caused by the deviation of the voltage or current amplitude applied to the excitation coil of the TOO from their nominal value. This deviation

has a negative effect on most of the characteristics of the TOO [16]. The deviation of the current in the excitation coil leads to the following change in the MMP in the magnetic circuit of the TOO:

$$\Delta U_{\mu\kappa} = \Delta I_{e\kappa} w_{\kappa}. \quad (32)$$

The relative error caused by the current deviation is determined as follows:

$$\gamma_{I_{e\kappa}} = \frac{\Delta I_{e\kappa}}{I_{e\kappa}} \cdot \Delta Q_M. \quad (33)$$

To reduce this error, it is recommended to supply the TOO excitation coil by means of voltage or current stabilizers.

2.4.2 Excitation Coil Current Frequency Error

Error caused by current frequency deviation in the TOO excitation coil. The output EMF of the TOOs supplied from the current source is written in the following general expression:

$$\dot{E}_{out.} = -j\omega \dot{I}_{e\kappa} M, \quad (34)$$

where M is the mutual inductance between the windings, [H].

If the reactive losses in the magnetic conductor (steel) are not taken into account, then the modulus value of the EMF at the output of the TOO can be expressed as follows:

$$E_{out.} = \omega I_{e\kappa} M. \quad (35)$$

It is known [6] that the error due to the deviation of the source frequency in the TOOs can be calculated using the following (36):

$$\gamma_{\omega} = \frac{1}{E_{out.max}} \cdot \frac{\partial E_{out.}}{\partial \omega} \Delta \omega = \frac{\Delta \omega}{\omega} \cdot \frac{M}{M_{max}} \cdot 100 \%. \quad (36)$$

Equation (36) it can be seen from the expression that the error caused by the frequency deviation decreases as the source current frequency increases. For the new TOEs under study, the value of this error is at the maximum value of the input magnitude, that is ΔQ_{Mmax} reaches the maximum. In the state standard, the industrial frequency is allowed to vary by a maximum of 0.2 Hz [14]. Therefore is in the range of $\gamma_{\omega} \leq 0,4 \%$.

2.4.3 Excitation Coil Current Distortion Error

Error caused by distortion of the current shape in the TOO excitation coil. The expression EMF in the

output band of the TOO operating in the straight-line part of the magnetization characteristic of the magnetic chain is written as follows [10]:

$$e_{out.} = -M \frac{di_{e\kappa}}{dt}. \quad (37)$$

If the current in the excitation coil contains high harmonic components, such as n -order harmonics, for other reasons not related to the properties of the magnetic circuit of the TOO, then (37) is written as follows:

$$e_{out.} = -\omega M (I_{e\kappa,m1} \cos \omega t + n I_{e\kappa,mn} \cos n \omega t). \quad (38)$$

For this case, the error due to the distortion of the current in the arrow drive is determined as follows:

$$\gamma_{\kappa,n} = n \frac{I_{e\kappa,mn}}{I_{e\kappa,m1}} \cdot \frac{\Delta Q_M}{\Delta Q_{Mmax}}. \quad (39)$$

2.5 External Additional Error Sources

If it is possible to reduce the internal sources of error by improving (stabilizing) the source parameters that provide the TOO, then its external sources depend on the environmental conditions in which the TOO operates, and it is not always possible to improve them.

2.5.1 Ambient Temperature Error

Error caused by changes in ambient temperature. The active resistances ($R_{e\kappa}$ and $R_{emeas.}$), Of the coils of the new TOOs under study change with ambient temperature, the specific magnetic resistance (ρ_{μ} of the magnetic conductor material and its geometric dimensions change according to the following laws [8]:

$$R_e = R_{e0} (1 + \alpha_R \Delta \theta), \quad (40)$$

$$Z_{\mu n} = Z_{\mu n0} \frac{(1 + \alpha_{\mu} \Delta \theta)}{(1 + \alpha_l \Delta \theta)}, \quad (41)$$

Where is $\alpha_R, [K^{-1}]$, $\alpha_{\mu}, [K^{-1}]$ and $\alpha_l, [K^{-1}]$ – temperature coefficients on electrical and magnetic resistances and expansion of the material, respectively; $\Delta \theta, [K]$ – the difference between the current and normal temperatures of the environment.

It is known that [14], the temperature coefficient TOO is found using the following:

$$\sigma_{\Delta \theta} = \frac{\partial E_{out.}}{\partial R_e} \cdot \frac{\partial R_e}{\partial \Delta \theta} + \frac{\partial E_{out.}}{\partial Z_{\mu n}} \cdot \frac{\partial Z_{\mu n}}{\partial \Delta \theta} + \frac{\partial E_{out.}}{\partial X_M} \cdot \frac{\partial X_M}{\partial \Delta \theta}. \quad (42)$$

If we take into account that the new TOOs under study are mainly supplied from the current source and the output size is considered to be induced EMF in the measuring circuit of the operating mode (the output of the TOO is often connected to an amplifier with very large input resistance), then the resistance of excitation and measuring. The effect on the characteristics can be ignored [12]. In addition, we do not take them into account due to the fact that the gains of the geometric dimensions of steel magnetic conductors in the magnetic circuit of the TOO are very small due to temperature changes. Given these limitations, (42) looks like this:

$$\sigma_{\Delta\theta} = \frac{\partial E_{out}}{\partial Z_{\mu n}} \cdot \frac{\partial Z_{\mu n}}{\partial \Delta\theta} = -\frac{\omega I_{ek} W_{\kappa} W_{meas} \Delta Q_M}{(Z_{\mu n} + Z_{\mu \delta})^2 \Delta Q_{Mmax}} Z_{\mu n 0} \alpha_{\mu}. \quad (43)$$

The error due to the change in the magnetic properties (relative magnetic permeability) of the magnetic conductive material when the ambient temperature changes is calculated according to the following (44):

$$\gamma_{Z_{\mu n}(\Delta\theta)} = -\frac{\Delta\theta}{E_{out,max}} \cdot \frac{\partial E_{out}}{\partial Z_{\mu n}} \cdot \frac{\partial Z_{\mu n}}{\partial \Delta\theta} = -\frac{\Delta Q_M \Delta\theta}{(Z_{\mu n} + Z_{\mu \delta}) \Delta Q_{Mmax}} Z_{\mu n 0} \alpha_{\mu}. \quad (44)$$

Equation (44) analysis shows that, ΔQ_M , $\Delta\theta$ and α_{μ} decreases with $Z_{\mu \delta}$ and with increasing of ΔQ_{Mmax} $\gamma_{Z_{\mu n}(\Delta\theta)}$ will decrease.

2.5.2 External Magnetic Field Error

Error caused by the effect of an external magnetic field. For the most unfavorable condition where the coupling current of the external magnetic field coincides with the coupling current of the working magnetic field in phase, direction and frequency, this error can be calculated using the following [11]:

$$\gamma_{Q_{\mu(\tau)}} = \frac{\Psi_{\tau}}{\Psi_w} = \frac{B_{\tau}}{B_w}. \quad (45)$$

The found value of the magnetic induction in the working air gap based on the static characteristics of the new TOO is equal to:

$$B_w = \frac{2I_{ek} W_{\kappa} W_{\mu \delta w 0}}{S_{\mu \delta w} [W_{\mu \delta w 0}^2 - K_1^2 (\Delta Q_M)^2]}. \quad (46)$$

Equation (46) shows that the error expression due to the effect of the external magnetic field is written as follows:

$$\gamma_{Q_{\mu(\tau)}} = \frac{B_{\tau} S_{\mu \delta w} [W_{\mu \delta w 0}^2 - K_1^2 (\Delta Q_M)^2]}{2I_{ek} W_{\kappa} W_{\mu \delta w 0}}. \quad (47)$$

Equation (47) analysis shows that in order to reduce this component of the error, it is necessary to increase the MMP of the excitation ring and reduce the value of the working air gap as much as possible.

2.5.3 External Ferromagnetic Mass Error

Error due to the effect of external ferromagnetic mass. An analysis of the literature devoted to the detection and evaluation of this error shows that [7], [11], [12], [15], its value is negligible. However, in order to have a general idea of this error, we cite additional EMF and error expressions that occur due to the effect of an external ferromagnetic mass:

$$\Delta \dot{E}_{out.(f.m.)} = -j\omega I_{ek} W_{\kappa} \frac{g_s}{2} X_M^2, \quad (48)$$

$$\gamma_{f.m.} = \frac{X_M}{2C_{\mu \delta w}} \cdot C_{\mu s} = \frac{X_M}{2C_{\mu \delta w}} \cdot \mu_0 \frac{h_x + bk_s}{h_s}. \quad (49)$$

Where is $C_{\mu s} = \mu_0 \frac{h_x + bk_s}{h_s}$ – the air gap between the arrow and the external ferromagnetic mass is the pogan value of the magnetic capacity; X_M – the length of the working part of the Archimedean spiral; $C_{\mu \delta w}$ – the magnetic capacity of the working air gap; h_s – TOO the distance between the annular magnetic conductor and the external ferromagnetic mass; k_s – proportionality coefficient.

Equation (49) analysis shows that in order to reduce the error due to the effect of the external ferromagnetic mass, it is necessary to increase the distance between the TOO and the external ferromagnetic mass and increase the magnetic capacity of the working air gap.

2.6 Operating Mode Dependent Error Sources

2.6.1 Load Change Error

Error caused by load change. As mentioned above, although the output of the MD is often connected to an amplifier with a very large input resistance, in some cases it can also be connected directly to a load with a known resistance.

In order to derive the formula for calculating the error caused by the change in load, we find the modulus value of the load current of the TOOs under study. It will look like the following:

$$I_{load} = \frac{X_M U_{\kappa}}{\sqrt{Z_{\Sigma a}^4 + Z_{\Sigma p}^4}}. \quad (50)$$

Where is

$$\begin{aligned}
 Z_{\Sigma a}^4 &= R_{meas}^2 R_{\kappa}^2 + X_M^4 + 2X_M^2 R_{meas} R_{\kappa} - \\
 &2R_{meas} R_{\kappa} X_{\kappa} X_{meas} - 2X_M^2 X_{\kappa} X_{meas} + X_{\kappa}^2 X_{meas}^2 + \\
 &R_{b\kappa}^2 R_{\kappa}^2 + 2R_{load} R_{\kappa}^2 R_{meas} + 2X_M^2 R_{load} R_{\kappa} - \\
 &- 2R_{load} R_{\kappa} X_{\kappa} X_{meas} - 2X_{\kappa} X_{load} R_{meas} R_{\kappa} - (51) \\
 &2X_{\kappa} X_M^2 X_{load} + 2X_{\kappa}^2 X_{meas} X_{load} - 2X_{\kappa} X_{load} R_{load} R_{\kappa} + \\
 &X_{\kappa}^2 X_{load}^2, \\
 Z_{\Sigma p}^4 &= X_{meas}^2 R_{\kappa}^2 + X_{\kappa}^2 R_{meas}^2 + 2X_{\kappa} X_{meas} R_{\kappa} R_{meas} \\
 &+ X_{b\kappa}^2 R_{\kappa}^2 \\
 &+ 2X_{meas} X_{load} R_{\kappa}^2 + 2X_{\kappa} R_{meas} X_{load} R_{\kappa} \quad (52) \\
 &+ 2X_{\kappa} X_{meas} R_{\kappa} R_{load} + \\
 &+ 2X_{\kappa}^2 R_{meas} R_{load} + 2X_{\kappa} X_{load} R_{load} R_{\kappa} + X_{\kappa}^2 R_{load}^2,
 \end{aligned}$$

Where is R_{κ} , R_{meas} , R_{load} , X_{κ} , X_{meas} , X_{load} , X_M – active and reactive resistances of excitation, measuring coils and load, as well as mutual inductive resistance.

Equation (50) from the equation R_{load} and X_{load} respectively, we write the formulas for calculating the errors due to changes in the active and reactive components of the load as follows:

$$\begin{aligned}
 \gamma_{\Delta R_{load}} &= \frac{\Delta R_{load}}{I_{loadmax}} \cdot \frac{dI_{load}}{dR_{load}} = \\
 &\frac{\Delta R_{load} M (R_{load} R_{\kappa}^2 + R_{meas} R_{\kappa}^2 - X_{\kappa} X_{meas} R_{\kappa} - X_{\kappa} X_{load} R_{\kappa} + \\
 &M_{max} \sqrt{\frac{(Z_{\Sigma a}^4 + Z_{\Sigma p}^4)^3}{Z_{\Sigma a}^4 Z_{\Sigma a}^{max} + Z_{\Sigma p}^4 Z_{\Sigma p}^{max}}}}{\Delta R_{load} M (R_{load} R_{\kappa}^2 + R_{meas} R_{\kappa}^2 - X_{\kappa} X_{meas} R_{\kappa} - X_{\kappa} X_{load} R_{\kappa} + \\
 &+ X_M^2 R_{\kappa} + X_{\kappa}^2 R_{load} + X_{\kappa} X_{meas} R_{\kappa} + X_{\kappa}^2 R_{meas} + X_{\kappa} X_{load} R_{\kappa})} \quad (53) \\
 &\rightarrow \frac{\Delta X_{load}}{I_{loadmax}} \cdot \frac{dI_{load}}{dX_{load}} = \\
 &\frac{\Delta X_{load} M (X_{load} R_{\kappa}^2 - R_{meas} R_{\kappa} X_{\kappa} - X_M^2 X_{\kappa} - X_{\kappa} R_{load} R_{\kappa} + \\
 &M_{max} \sqrt{\frac{(Z_{\Sigma a}^4 + Z_{\Sigma p}^4)^3}{Z_{\Sigma a}^4 Z_{\Sigma a}^{max} + Z_{\Sigma p}^4 Z_{\Sigma p}^{max}}}}{\Delta X_{load} M (X_{load} R_{\kappa}^2 - R_{meas} R_{\kappa} X_{\kappa} - X_M^2 X_{\kappa} - X_{\kappa} R_{load} R_{\kappa} + \\
 &+ X_{\kappa}^2 X_{meas} + X_{\kappa}^2 X_{load} + X_{meas} R_{\kappa} R_{\kappa} + X_{\kappa} R_{meas} R_{\kappa} + X_{\kappa} R_{load} R_{\kappa})} \quad (54)
 \end{aligned}$$

Where $I_{loadmax}$, $Z_{\Sigma a}^4$ and $Z_{\Sigma p}^4$ are taken from the form.

In (50), instead of L_{κ} , L_{meas} and M and M , their maximum values are $L_{\kappa,max}$, $L_{meas,max}$ and M_{max} placed respectively.

Analysis of (53) and (54) shows that a change in the active component of the load resistance produces more errors than a change in the reactive component of its inductive nature.

2.6.2 Dynamic Movement Error

Error caused by dynamic movements of moving parts of TOO. This component of the additional error is the dynamic error [7]. We find the difference in the angle of rotation of the moving parts of the bullet $\Delta Q_M = \Delta Q_{Mmax} \sin \Omega_M t$ we define

the error expression for a situation that varies according to the law.

For the case where the magnetic resistance of the magnetic conductor (steel) under study is not taken into account, the induced EMF in the measuring vessel is written as follows:

$$\begin{aligned}
 e_{out} &= w_{meas} \cdot \frac{\partial}{\partial t} Q_{\mu,meas} = \\
 w_{\kappa} w_{meas} C_{\mu \Sigma} I_{e\kappa} \Delta Q_{Mmax} (\omega_e \cos \omega_e t \cdot \sin \Omega_M t + \\
 &+ \Omega_M \sin \omega_e t \cdot \cos \Omega_M t). \quad (55)
 \end{aligned}$$

Equation (55) the first component of the expression is the transformer (useful) EMF, the maximum value of which corresponds to the value of the input magnitude $\Delta Q_M = \Delta Q_{Mmax}$, and the second component of the expression is the generator (interference) EMF, the maximum value of which will be at $\Delta Q_M = 0$.

The ratio of the maximum value of the generator EMF to the maximum value of the transformer EMF describes the error caused by the dynamic movements of the moving parts of the MD:

$$\gamma_{\Omega_M} = \frac{\Omega_M}{\omega_e} \quad (56)$$

3 RESULTS AND DISCUSSION

The formulas of theoretical calculation of sources of error of measuring transformers distinguishing all types of angular displacements are given above. Evaluation of regular and random errors of new transformer converters measuring angular displacement difference.

The theoretical, technological, and operational components of the above error sources are routine errors, and internal, external, and regime sources are random errors.

The systematic error of the TOO (γ_M) is determined in the form of an algebraic sum of its constituents (γ_{mk}) using the following [1]:

$$\gamma_M = \sum_{k=1}^m \gamma_{mk} \quad (57)$$

Due to the non-linearity of static characteristics in theoretical sources of error, the existing new transformer increased the converter working air interval by 2 mm to 1,09%. And the error caused by the reactive component of the magnetic resistance of the magnetic conductor was reduced to 0,063%, changing the dimensions and design parameters of the maintenance.

The errors arising from inaccuracies in the assembly and configuration of the design in the

sources of technological errors amounted to 0,033% for the design parameters of the new TOO. In this case, the systematic errors of TOO

$$\gamma_M = \sum_{k=1}^m \gamma_{Mk} = 1,186\%. \quad (58)$$

Random error of TOO γ_T is determined as the sum of mean square values of its components γ_{Ti} by [2]:

$$\gamma_T = \sqrt{\sum_{i=1}^n \gamma_{Ti}^2}. \quad (59)$$

At the same time, the errors contained in the internal sources of additional error were minimized by extracting current or voltage from an ideal source, and the errors contained in the external sources of additional error were minimized by protecting (shielding) from the effect of an external magnetic field at normal temperature in the operating mode. Random error of new TOO

$$\gamma_T = \sqrt{\sum_{i=1}^n \gamma_{Ti}^2} = 0,31.$$

The total error TOO is determined as an algebraic sum of systematic and random errors in it:

$$\gamma_{yM} = \sum_{k=1}^m \gamma_{Mk} + \sqrt{\sum_{i=1}^n \gamma_{Ti}^2}. \quad (60)$$

The total error of the new TOO is

$$\gamma_{yM} = \sum_{k=1}^m \gamma_{Mk} + \sqrt{\sum_{i=1}^n \gamma_{Ti}^2} = 1,496.$$

The error of the new maintenance has decreased by 1,203 times compared to the error of the existing maintenance due to the improvement of the design and the correct choice of design parameters [3]. This decrease in the total error makes it possible to measure the difference in angular displacements of the two objects in the exact values in the control and monitoring systems.

4 CONCLUSIONS

Taking into account each parameter, structure, structure and external and internal effect of the transformer, which measures the difference in angular displacement, formulas have been created to calculate the transformer error. This, in turn,

makes it possible to theoretically calculate the error of each transformer and take measures to reduce the total error. It has been established that the working air space of transformers Transformer in theoretical sources of error, caused by the error of static characteristics, decreases with an increase in the value of magnetic stiffness. If the working air cell of the new transformer is 1 mm, then the error caused by its static characteristics is 2,67%, and if you select a working air cell of 2 mm, then the error will decrease by 2,5 times or 1,09%. It has been established that for the dimensions and design parameters of the new transformer, the error does not exceed 0,063% due to the reactive component of the magnetic resistance of the magnetic conductor. In addition, it was found that the fraction of the highest harmonic in the output voltage does not exceed the fraction of the 3rd harmonic in the 1st harmonic, taking into account the error arising from the high harmonic 4,8% of the output voltage of the converter. The most convenient way to reduce this proportion is to ensure that this part of the steel in the magnetic circuit operates on a straight section of the magnetic characteristic.

The error caused by inaccuracies in the assembly and configuration of the structure was 0,033% for the dimensions and design parameters of the new transformer.

It was found that the error value caused by play, mechanical hysteresis, magnetic hysteresis in the working air intervals of the sources of operational error does not exceed 0,0065% for the new transformer.

Errors arising from overvoltage or deviation of current amplitude from their nominal value, arising from the fact that new transformers cause an internal voltage contained in additional sources of error, and errors arising from deviation of current frequency in the pulse eliminating errors arising from violation of the current form by providing ideal sources of current and voltage. External sources include errors resulting from changes in ambient temperature, errors resulting from exposure to an external magnetic field, and errors resulting from exposure to an external ferromagnetic mass.

The new modifiers showed that the errors arising from weak static characteristics are larger compared to other main sources, and the errors arising from changes in amplitude, frequency and load resistance are larger compared to other additional sources, and the new transformer converters are not more than 1,5%.

REFERENCES

- [1] C. Rui, L. Hongwei, and T. Jing, "Structure design and simulation analysis of inductive displacement sensor," in Proc. 13th IEEE Conf. on Industrial Electronics and Applications (ICIEA), 2018; see also R. Malaric, *Instrumentation and Measurement in Electrical Engineering*. Irvine, CA, USA: Universal-Publishers, 2011, 244 p.
- [2] Patent of the Republic of Uzbekistan UZ IAP 06642, "Transformer converter of angular displacements," S. F. Amirov, N. R. Yuldashev, S. Kh. Zhumaboev, and Zh. S. Faizullaev, *Official Newsletter*, no. 1, 2022.
- [3] A. A. Trofimov, "Methodical error in calculating magnetic fluxes of transformer displacement sensors," *Measurement. Monitoring. Management. Control.*, no. 4 (6), pp. 9–15, 2013.
- [4] M. Bazarov, I. M. Bedritskiy, and O. T. Boltaev, "Estimation of an error of calculations of ferromagnetic elements from inductance of dispersion," *European Journal of Technical and Natural Sciences*, no. 3, pp. 47–49, 2017.
- [5] N. R. Yusupbekov, Kh. Z. Igamberdiev, and A. V. Malikov, *Fundamentals of Automation of Technological Processes*, vol. 2, parts 1–2. Tashkent, Uzbekistan: TSTU, 2007, 152 p., 173 p.
- [6] M. Yakubov, A. Sulliev, and A. Sanbetova, "Modern methods of evaluation of metrological indicators of channels for measurement and processing of diagnostic values of traction power supply," *IOP Conf. Series: Earth and Environmental Science*, vol. 1142, no. 1, Art. no. 012010, 2023.
- [7] X. Gu, Q. Tang, D. Peng, and D. Weng, "An inductive linear displacement sensor with bilateral sensing units," *IEEE Sensors Journal*, vol. 21, no. 1, pp. 296–305, 2021.
- [8] S. Zheng, X. Liu, Y. Zhang, B. Han, Y. Shi, and J. Xie, "Temperature drift compensation for exponential hysteresis characteristics of high-temperature eddy current displacement sensors," *IEEE Sensors Journal*, vol. 19, no. 23, pp. 11041–11049, 2019.
- [9] I. Siddikov, M. Sobirov, A. Abdumalikov, and K. Sattarov, "Equipment and software for energy supply monitoring and control process," in Proc. Int. Conf. on Information Science and Communications Technologies (ICISCT), 2021, p. 202.
- [10] K. R. Sandra, A. S. A. Kumar, B. George, and V. J. Kumar, "A linear differential inductive displacement sensor with dual planar coils," *IEEE Sensors Journal*, vol. 19, no. 2, pp. 457–464, 2019.
- [11] V. Goodship, A. Stevels, and J. Huisman, *Waste Electrical and Electronic Equipment (WEEE) Handbook*. Oxford, U.K.: Elsevier, 2012, 752 p.
- [12] N. Anandan and B. George, "Design and development of a planar linear variable differential transformer for displacement sensing," *IEEE Sensors Journal*, vol. 17, no. 16, pp. 5298–5305, 2017.
- [13] S. Amirov, D. Rustamov, N. Yuldashev, U. Mamadaliev, and M. Kurbanova, "Study on the electromagnetic current sensor for traction electro supply devices control systems," *IOP Conf. Series: Earth and Environmental Science*, vol. 939, Art. no. 012009, 2021.
- [14] L. Wu, S. Xu, Z. Zhong, C. Mou, and X. Wang, "An inductive sensor for two-dimensional displacement measurement," *Sensors*, vol. 20, no. 7, Art. no. 1819, Mar. 2020.
- [15] C. Chiriac and H. Chiriac, "Magnetic field and displacement sensor based on linear transformer with amorphous wire core," *Sensors and Actuators A: Physical*, vol. 106, nos. 1–3, pp. 172–173, Sep. 2003.